Measurement of vibroacoustical energy flow through straight pipes

nederlands akoestisch genootschap
NAG

journaal
nr. 114
september 1992

MEASUREMENT OF VIBROACOUSTICAL ENERGY FLOW THROUGH STRAIGHT PIPES

ir. C.A.F. de Jong[1], prof.dr.ir. J.W. Verheij[1] and ir. M.H.J. Bakermans[2]
1: TNO Institute of Applied Physics, P.O. Box 155, 2600 AD Delft
2: now at : DGMR, Eisenhowerlaan 112, 2517 KM Den Haag

Summary: The measurement of vibroacoustical energy flow through straight pipes has been investigated. At frequencies below the cut-on of n=3 shell waves the energy propagates in a limited number of waves. The structure-borne energy in these waves can be determined from acceleration measurements on the pipe surface, provided that appropriate accelerometer configurations are chosen to separate the different waves. The energy flow in each wave can then be determined using a two-channel cross-spectral density method. It appears to be impossible to determine the fluid-borne energy flow from acceleration measurements, due to the transverse axis sensitivity of the accelerometers. Experiments on a cooling water pipe of a shipboard diesel engine indicate that energy flow measurements are feasible, although further investigations are necessary to achieve a practicable and reliable method.

Nomenclature

a	mean pipe radius
D	membrane stiffness of the shell
E_s	Young's modulus of the shell material
f_{cn}	cut-on frequency for mode n>1
h	shell thickness
I_x	axial component of intensity
k	wavenumber
n	circumferential mode number
N	thin shell resultant force
p	acoustical pressure in the fluid
P_x	axial energy flow
r	radial coordinate
u	axial shell displacement
v	tangential shell displacement
v_x	axial acoustical velocity in the fluid
w	radial shell displacement
x	axial coordinate
β^2	shell thickness parameter $h^2/12a^2$
Δx	axial distance
θ	circumferential angle
ν	Poisson ratio

subscripts

f,s	fluid, shell
x,r,θ	axial, radial, circumferential
n	circumferential mode
B,L	bending, lobar mode
S,F,T	longitudinal, fluid, torsional mode

1 INTRODUCTION

The amount of vibroacoustical energy that is transported along a certain sound path can be used to quantify the relevance of that path for the total sound transfer. In many practical situations pipes form connections between noisy sources (engines, pumps) and locations where excessive sound levels should be avoided. In order to determine the sound transfer to a receiver position, measurements of energy flow on the pipe near the source have to be combined with — reciprocal — measurements of the transfer function from energy flow to sound power at the receiver position [1], which might involve direct radiation from the pipe but also radiation from plate structures that are excited by the pipe through pipe foundations.

In this paper we will describe how to measure the energy flow along fluid-filled pipes. Theoretical study of the vibroacoustical energy transfer along straight pipes leads to the formulation of a practical measurement method. The practicability of this method is investigated through measurements on a cooling water pipe of a shipboard diesel generator.

2 DEFINITION OF ENERGY FLOW

The definition of vibroacoustical energy flow through straight pipes has been covered extensively in the literature of the last ten years [2–5]. For practical application only the axial energy flow through pipes has to be considered. The total axial energy flow P_x is the sum of the fluid-borne energy flow P_{xf} and the structure-borne energy flow P_{xs}. Figure 1 shows the geometry of a pipe. For pipes the ratio of wall thickness h to mean radius a is generally small (h/a<0.1) so that they can be described as thin walled shells.

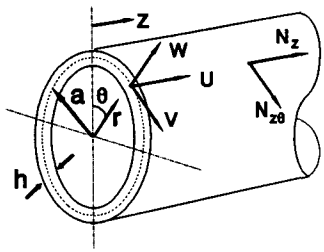

Figure 1 Shell geometry, displacements and forces.

2.1 Fluid-borne energy flow

The definition of fluid-borne energy flow is derived by integration from the definition of acoustical intensity as the time averaged product of pressure p and particle velocity v_x [2]:

$$P_{xf} = \int_0^{2\pi} \int_0^a < p v_x >_t \; r \; dr \; d\theta \tag{1}$$

where the particle velocity is related to an axial pressure gradient by the Euler equation:

$$\frac{\partial v_x}{\partial t} = -\frac{1}{\rho_f} \frac{\partial p}{\partial x} \tag{2}$$

2.2 Structure-borne energy flow

In a thin walled shell the vibrational energy is carried almost entirely by extensional and torsional stretching motion [2,6]. Radial shear stresses and bending and twisting moments of the shell are proportional to $\beta^2=h^2/12a^2$ and therefore much smaller than the longitudinal and tangential shear stresses. The total axial structure-borne energy flow may be expressed in terms of the classical resultant forces $N_x, N_{x\theta}$ and of the three-dimensional displacements u,v,w of the mid-surface of the shell (fig. 1), where the dot

denotes a time derivative:

$$P_{xs} = -\int_0^{2\pi} < N_x \dot{u} + N_{x\theta} \dot{v} >_t \; a \; d\theta \tag{3}$$

Using the stress-strain relationships from the Donnell-Mushtary shell theory [6], the forces can be written in terms of shell displacements:

$$N_x = D\left(\frac{\partial u}{\partial x} + \nu\left(\frac{1}{a}\frac{\partial v}{\partial \theta} + \frac{w}{a}\right)\right), \; N_{x\theta} = \frac{1-\nu}{2} D\left(\frac{\partial v}{\partial x} + \frac{1}{a}\frac{\partial u}{\partial \theta}\right) \tag{4}$$

where D is the membrane stiffness of the shell: $D=E_s h/(1-\nu^2)$.

3 WAVE DECOMPOSITION

The vibroacoustical energy is transported through the pipe by propagating waves. At frequencies that are of practical interest only a limited number of waves can propagate along the pipe.

3.1 Circumferential modes and cut-on frequencies

Due to the circular symmetry, wave propagation occurs in circumferential modes of various orders n, with modeshapes as shown in figure 2. The shell displacements u,v,w and the acoustic pressure p can be expanded in these modes [2,4,6]. Waves for n>1 show cut-on frequencies f_{cn}, so that no wave of mode n can propagate at frequencies below f_{cn}. An important frequency range is covered if we consider frequencies below f_{c3} only. The total energy flow is then obtained by summation of modes. Intermodal cross terms do not contribute to the integral [4], so that the total energy flow can be written as:

$$P_x = \sum_{n=0}^{2} [(P_{xs})_n + (P_{xf})_n] \tag{5}$$

Each mode n has its own modal amplitudes $u_n(x,t), v_n(x,t), w_n(x,t)$ and $p_n(x,r,t)$ and polarization angles $\theta_n(x,t)$, which for unidirectional propagating waves are related by the equations of motion of shell and fluid. Multiple axial waves correspond to each circumferential mode n. However, in pipes that are long compared to the axial wavelength only the waves with a real axial wavenumber k are of interest for the energy flow, because complex wavenumbers are associated with exponentially decaying waves. The technique for experimental wave decomposition is based on the assumption that each wave has its most characteristic wall displacement so that the energy flow can be derived from acceleration measurements on the pipe wall.

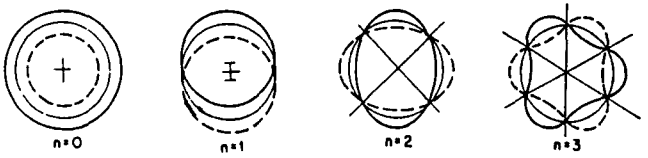

Figure 2 Radial modeshapes for n=0, n=1, n=2 and n=3.

3.2 Experimental decomposition using accelerometers

Below the cut-on of n=3 waves the circumferential modes can be separated easily, thanks to the simple θ-dependence of the shell displacements. For example:

$$\ddot{u}(x,t) = \ddot{u}_0(x,t) + \ddot{u}_1(x,t)\cos[\theta + \theta_1(x,t)] + \ddot{u}_2(x,t)\cos[2\theta + \theta_2(x,t)] \qquad (6)$$

Three amplitudes and two phase angles have to be determined from measurements. This means that the shell displacement should be measured at five circumferential positions at least. In practice the modal accelerations and polarization angles are determined according to figure 3:

$$\ddot{u}_0 = \frac{1}{4}(\ddot{u}_A + \ddot{u}_B + \ddot{u}_C + \ddot{u}_D),\ \ddot{v}_0 = \frac{1}{4}(\ddot{v}_A + \ddot{v}_B + \ddot{v}_C + \ddot{v}_D),\ \ddot{w}_0 = \frac{1}{4}(\ddot{w}_A + \ddot{w}_B + \ddot{w}_C + \ddot{w}_D)$$

$$\ddot{w}_1\cos(\theta_1) = \frac{1}{2}(\ddot{w}_A - \ddot{w}_C),\ \ddot{w}_1\sin(\theta_1) = \frac{1}{2}(\ddot{w}_B - \ddot{w}_D) \qquad (7)$$

$$\ddot{w}_2\cos(\theta_2) = \frac{1}{4}(\ddot{w}_A - \ddot{w}_B + \ddot{w}_C - \ddot{w}_D),\ \ddot{w}_2\sin(\theta_2) = \frac{1}{4}(\ddot{w}_{A'} - \ddot{w}_{B'} + \ddot{w}_{C'} - \ddot{w}_{D'})$$

Four accelerometers at 90° angle are used for the n=0 and n=1 modes. The amplitude and the polarization angle of the n=2 mode is determined after rotating the set of accelerometers over 45°. The advantage of using eight circumferential positions instead of five is that the decomposition can be performed with simple hardware addition and subtraction devices [7,8,9], thus reducing the number of signals which need to be processed.

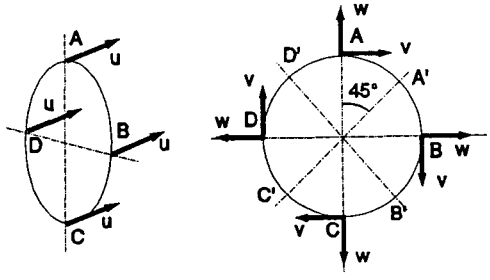

Figure 3 Accelerometer configurations for cirumferential mode separation.

3.3 Wave decomposition at n=0

Three propagating waves occur at n=0: a torsional wave ('T') which is determined by the torsional displacement v_0, a quasi-longitudinal extensional wave ('S') in the wall, coupled to fluid motion via Poisson contraction, and a plane pressure wave ('F') in the fluid that is coupled to a radial 'breathing' shell motion. Figure 4 shows the u_0 over w_0 ratio for the coupled waves.

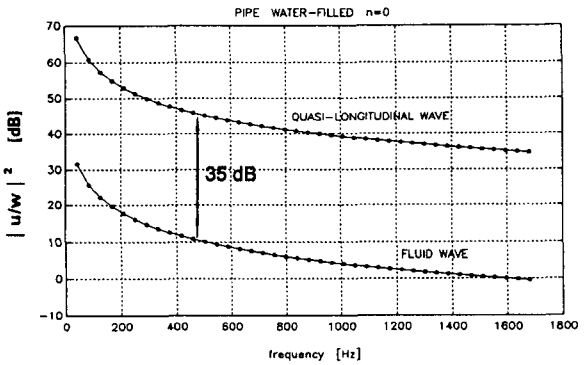

Figure 4 Amplitude relationship u/w for n=0 waves in the cooling water pipe.

The shell is so stiff in circumferential direction that the axial motion predominates for both waves. In practice, where it is not always possible to measure the pressure inside pipes — cutting holes is not always allowed —, the energy flow must be determined from acceleration measurements on the pipe wall. These measurements will be influenced by the simultaneous presence of the two coupled n=0 waves. Table I shows the relationship between the ratio of both energy flows and the amplitude ratios for unidirectional propagating waves:

Table 1 Ratio of fluid- to structure-borne energy flow in relationship to the displacement amplitude ratios for both waves in the cooling water pipe.

P_F/P_S [dB]	–20	–10	0	10	20
w_F^2/w_S^2 [dB]	–5	5	15	25	35
u_S^2/u_F^2 [dB]	40	30	20	10	0

This means that the error in the measurement of the radial displacement w_F^2 due to the presence of w_S^2 is smaller than 5% only if the fluid-borne energy flow P_F is 10 dB greater than the structure-borne energy flow P_S. Reversely the error in the measurement of u_S^2 is smaller than 5% if P_S is 5 dB greater than P_F. Note that these considerations are based on the displacement amplitudes of unidirectional propagating waves. In practice there will be partial standing wave patterns due to reflections in the pipe that differ for both n=0 waves. In that case the situation is much more complicated and highly dependent on the measurement positions relative to the standing wave field.

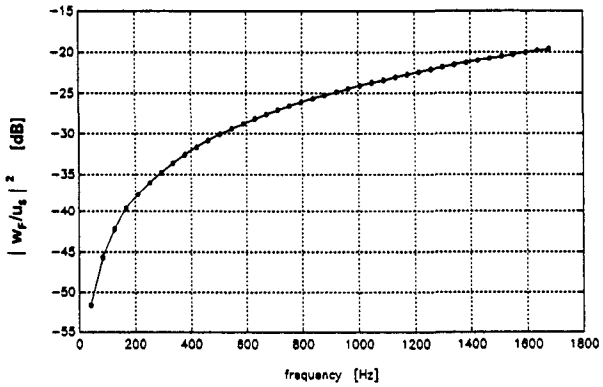

Figure 5 Ratio of the radial displacement w_F due to pressure in the fluid to the axial displacement u_S due to longitudinal extension of the wall if the energy flow in both waves in the cooling water pipe is equal.

Moreover there is the difficulty of the inherent transverse axis sensitivity of accelerometers which causes a coherent noise in the measurement of $\ddot{w}_F$ due to $\ddot{u}_S$. Figure 5 shows w_F over u_S if the energy flow in the two unidirectional travelling waves is equal. Considering that a transverse axis sensitivity of –30 dB is quite good for an accelerometer, it can be seen that it is impossible to determine the internal pressure from pipe wall accelerations in this case.

If it is not possible to apply pressure transducers in the pipe to determine the fluid-borne energy flow, the application of a circumferential piezoelectric transducer [10] or a more elaborate combination of sensors [5] might offer a solution.

The energy flow in the quasi-longitudinal wave can probably be determined from axial accelerations, provided that the energy flow in the fluid is not dominating.

3.4 Wave decomposition at n=1 and n=2

At n=1 and n=2 just one propagating wave occurs. For n=1 this wave is similar to a bending wave in a beam, while the n=2 lobar wave is characteristic for cylindrical shells. For both n=1 and n=2 there is an exponentially damped nearfield that occurs near discontinuities, like bends, flanges, etc. This means that a sufficient length of pipe should be available so that the measurements are not disturbed by the presence of nearfields. The wall acceleration for n=1 and n=2 is predominantly radial. The energy flow is equally due to axial extension and tangential shear as can be seen in figure 6, that shows the energy flow contributions as calculated for an unidirectional propagating wave. There it can also be seen that the corresponding fluid-borne energy flow is negligible, as is the energy flow due to local bending. The latter is shown to confirm the assumption that was made in deriving eq.(3).

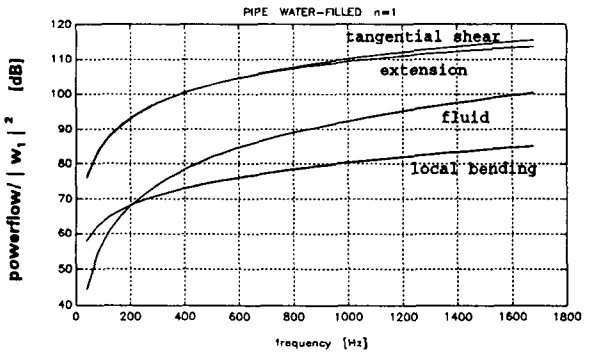

Figure 6 Contributions to the energy flow per radial displacement for n=1 bending waves in the cooling water pipe.

4 CROSS-SPECTRAL DENSITY METHOD

Assuming that the a decomposition of the different waves at a pipe cross-section can be made the energy flow per wave can be derived from the imaginary part of the cross-spectral density of accelerations — or pressures — at two closely spaced cross-sections [7]. This method involves the determination of the spatial derivative in eqs.(2) and (4) using a finite difference method. As in the two-microphone technique for measuring airborne sound intensity the distance between the two cross-sections should be small compared to the wavelength, but large enough to show significant phase differences.

5 INSTRUMENTATION

The phase differences between conditioned signals that have to be measured to determine energy flow may be very small. Therefore a high quality instrumentation is indispensable.

5.1 Accelerometers and studs

The accelerometers are mounted on the pipe using special made aluminium studs as shown in figure 7. It can be shown that a high stiffness of the glue with which the studs are mounted on the pipe surface and a well defined layer thickness are highly relevant for accurate phase measurements. Accelerometers of the type B&K 4382 (Delta-shear design) are used. The maximum transverse axis sensitivity of these accelerometers is 3% or less. Misplacement of the accelerometer, with its main axis not exactly normal or parallel to the pipe surface, may cause similar problems as the transverse axis sensitivity. The placement should be accurate within 1°. Accelerometer pairs are selected to be well matched (i.e. level difference of sum and difference signals > 60 dB at 80 Hz on a B&K 4291 calibrator).

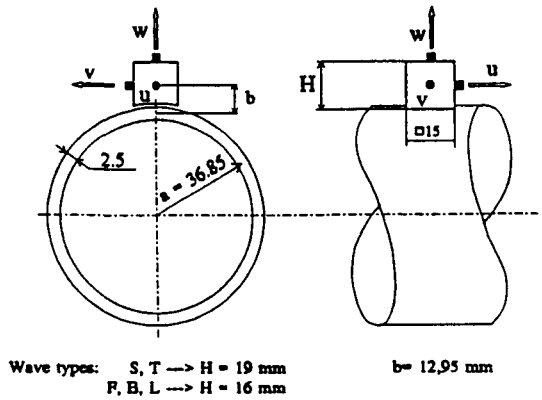

Figure 7 Aluminium accelerometer stud on the CuNiFer cooling water pipe.

5.2 Signal conditioning

Figure 8 shows a block diagram of the signal conditioning. Analogous add/subtraction devices are used for the circumferential mode decomposition, so that a two-channel measurement, similar to an acoustic intensity measurement, remains for each wave. The total instrument channel phase mismatch is calibrated and the measurement data are compensated for this mismatch.

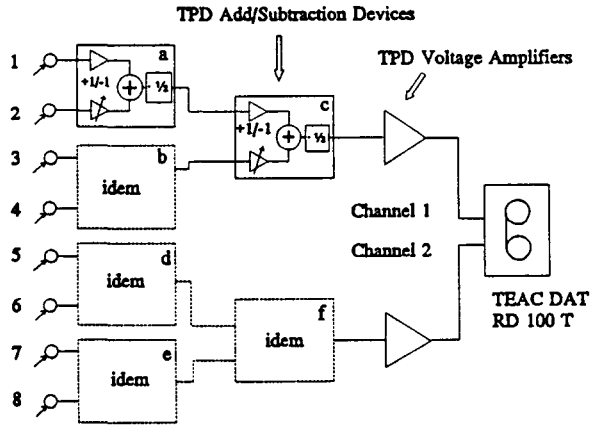

Figure 8 Block diagram of the instrumentation.

6 MEASUREMENTS AND RESULTS

Measurements have been performed on an inlet seawater cooling pipe of a shipboard auxiliary diesel engine. The engine was running at a constant speed (898 rpm) and load (275 kW) over the period of the whole measurement programme (about 10 hours). The dimensions of the CuNiFer cooling water pipe are shown in figure 7. Three measurement cross-sections were chosen (fig. 9): Cross-sections A and B on the same straight pipe and an extra cross-section C on a short pipe between two bends to check the method in a situation where nearfields might influence the measurements. A single accelerometer close to cross-section A was monitored during the whole measurement period to check the stability of the engine. The 1/3-octave band levels show a very stable response for most frequency bands, indicating that the successive measurements of the different energy flow contributions give a reliable picture of the total energy flow.

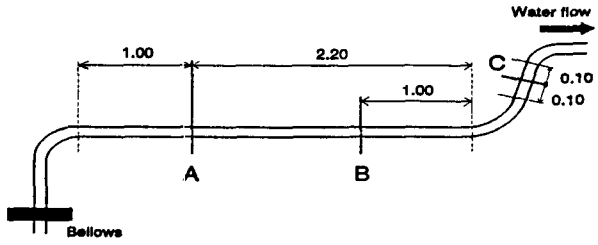

Figure 9 Measurement cross-sections on the cooling water pipe. Accelerometer spacings: $\Delta x_B=\Delta x_L=0.12$ m and $\Delta x_S=\Delta x_T=0.65$ m (A,B), $\Delta x_S=\Delta x_T=0.20$ m (C).

6.1 Acceleration response at a pipe cross-section

Figure 10 shows the acceleration response for the different waves at cross-section A in 1/3-octave bands. The cut-on of the n=2 waves in the 800 Hz-band can be seen clearly. At lower frequencies the response for n=2 is determined by transverse axis sensitivity of the accelerometers. The same low levels are observed for the fluid wave, showing that the energy flow in this wave can not be detected using accelerometers.

6.2 Energy flow

The energy flow in the different waves at cross-section A, presented in 1/1-octave bands to reduce information, is shown in figure 11. On average the structure-borne energy flow in torsional, quasi-longitudinal and bending waves is of the same order of magnitude. The energy flow in the n=2 lobar wave appears to be small compared to the other waves. Dots indicate an energy flow that is directed towards the diesel engine. Although there is no source to be responsible for such energy flows, these 'negative' energy flows might be caused by wave conversion at a discontinuity. The total structure-borne energy flow as determined for the three measurement cross-sections is shown in figure 12. As there is no cause for significant dissipation or wave conversion between cross-sections A and B, the energy flow levels should be equal. The differences that can be seen in figure 12 appear to

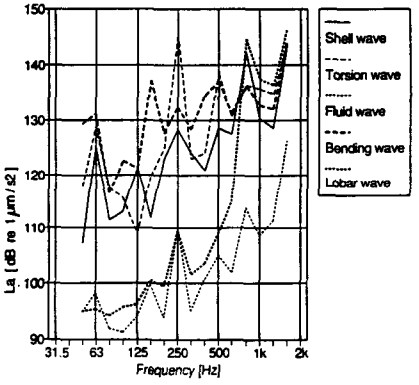

Figure 10 Acceleration response per wave at cross-section A in 1/3-octave bands.

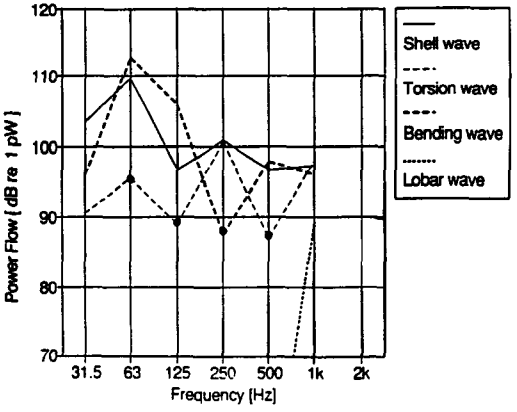

Figure 11 Octave band energy flow levels at cross-section A. Dots indicate energy flow towards the diesel engine.

be caused by the occurrence of 'negative' components in the energy flow. This effect has not yet been explained. Tests on the influence of phase errors — up to 0.5° — and of random errors — governed by the coherence function — did not provide sufficient explanation of the discrepancies found between A and B. The energy flow as determined on cross-section C, where nearfield effects are important, are much higher than those on A and B and therefore probably inaccurate. A further investigation on measurements on short pipe sections is highly relevant for practical application of the method.

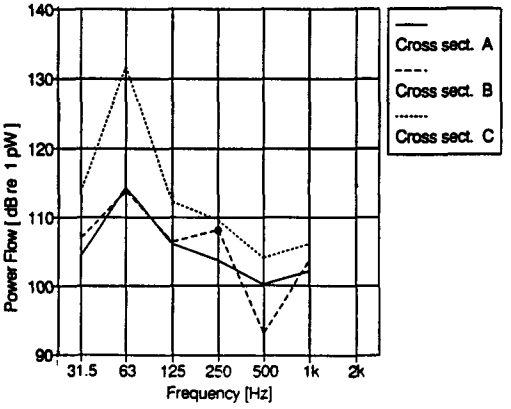

Figure 12 Octave band levels of total structural energy flow at three cross-sections. The dot indicates energy flow towards the diesel engine.

7 CONCLUSIONS

The development of a measurement method for vibroacoustical energy flow along a straight pipe — a relatively simple, unidirectional sound path — involves a thorough knowledge of the vibratory behaviour of the pipe. The method that is described here demands high quality instrumentation for reliable wave separation and accurate phase measurements. For the measurement of structure-borne energy flow these requirements can be met, provided that a straight pipe of sufficient length is available. Fluid-borne energy flow can not be determined from acceleration measurements on the pipe surface. Although a number of problems need further investigation energy flow measurements on pipes seem feasible.

References

1. J.W. Verheij, 1982. *Multi-path sound transfer from resiliently mounted shipboard machinery*, PhD Thesis, TNO Institute of Applied Physics, Delft.
2. C.R. Fuller & F.J. Fahy, 1982. Characteristics of wave propagation and energy distribution in cylindrical elastic shells filled with fluid, J. Sound and Vib. **81**(4), 501-518.
3. E.G. Williams, 1991. Structural intensity in thin cylindrical shells, J.Acoust.Soc.Am. **89**(4), 1615-1622.
4. G. Pavic, 1990. Vibrational energy flow in elastic circular cylindrical shells, J. Sound and Vib. **142**(2), 293-310.
5. G. Pavic, 1992. Vibroacoustical energy flow through straight pipes, J. Sound and Vib. **143**(3), 1992, 411-429.
6. A.W. Leissa, 1973. Vibration of shells, NASA SP-288, Washington DC.
7. J.W. Verheij, 1980. Cross spectral density methods for measuring structure-borne power flow on beams and pipes, J. Sound and Vib. **70**(1), 133-138.

8. J.W. Verheij, 1990. Measurements of structure-borne wave intensity on lightly damped pipes, Noise Control Engineering Journal, 35(2), 69-76.
9. C.A.F. de Jong & J.W. Verheij, 1992. Measurement of energy flow along pipes, *Second international congress on recent developments in air- and structure-borne sound and vibration*, Auburn University, 577-584.
10. R.J. Pinnington & A. Briscoe, 1992. Using a circumferential transducer to measure internal pressures within a pipe, *Second international congress on recent developments in air- and structure-borne sound and vibration*, Auburn University, 829-836.